



Cosmological observations to shed light on possible variations

expectations, limitations and status quo

M. Wendt¹ D. Reimers¹ and P. Molaro²

¹ Hamburger Sternwarte, Universität Hamburg, Gojenbergsweg 112, 21029 Hamburg, Germany e-mail: mwendt@hs.uni-hamburg.de

² Osservatorio Astronomico di Trieste, Via G. B. Tiepolo 11, 34131 Trieste, Italy

Abstract. Cosmology contributes a good deal to the investigation of variation of fundamental physical constants. High resolution data is available and allows for detailed analysis over cosmological distances and a multitude of methods were developed. The raised demand for precision requires a deep understanding of the limiting errors involved. The achievable accuracy is under debate and current observing proposals max out the capabilities of today's technology. The question for self-consistency in data analysis and effective techniques to handle unknown systematic errors is of increasing importance. An analysis based on independent data sets is put forward and alternative approaches for some of the steps involved are introduced.

Key words. Cosmology: observations – quasars: absorption lines – quasars: individual: Q0347-383 – cosmological parameters

1. Introduction

This work is motivated by numerous findings of different groups that partially are in disagreement with each other. A large part of these discrepancies reflect the different methods of handling systematic errors. Evidently systematics are not yet under control or fully understood. We try to emphasize the importance to take these errors, namely i.e. calibration issues, into account and put forward some measures adapted to the problem.

2. Data

2.1. Observations

Q0347-383 is one of the few quasars with an absorption spectrum that shows unblended strong features of molecular hydrogen. With a redshift of $z_{\text{abs}} = 3.025$ the UV transitions are shifted into a spectral range that can be observed with earthbound telescopes, rendering it an applicable target for $\Delta\mu/\mu$ analysis. Hence, Q0347 was subject of several works including the paper by Reinhold et al. (2006) that indicated a variation in μ and follow up papers by King et al. (2008), Wendt & Reimers (2008) and Thompson et al. (2009) which re-

Send offprint requests to: M. Wendt

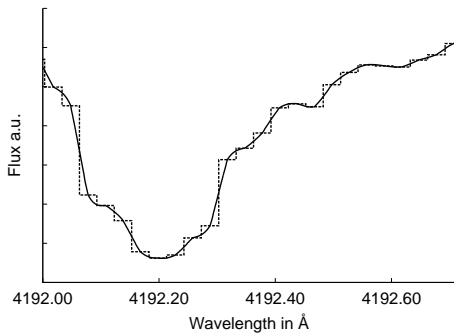


Fig. 1. The original flux is interpolated by a polynomial using *Neville's algorithm* to conserve the local flux.

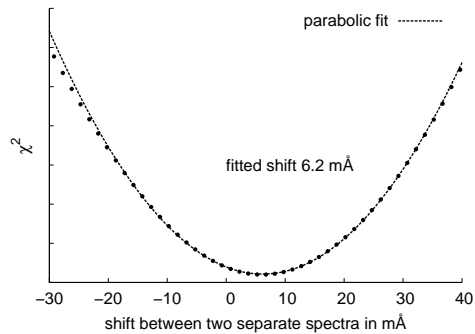


Fig. 2. Exemplary plot of the sub-pixel cross-correlation. The resulting shift is ascertained via parabolic fit. In this case the two spectra are in best agreement with a relative shift of 6.2 mÅ.

evaluated the data and report a result in agreement with no variation. All recent works on Q0347 are based on the same UVES VLT observations¹ in January 2002 (Ivanchik et al. 2005). For the first time additional observational data of Q0347 is taken into account in this work. The data were acquired in 2002 at the same telescope and recently reduced by Paolo Molaro².

2.2. Reduction

The standard UVES pipeline may not reach the desired accuracy for precise determination of fundamental physical constants. A major source of uncertainty are the calibration spectra and the limited precision of the available list of Thorium Argon lines as pointed out by Murphy et al. (2008) and Thompson et al. (2009). Proper calibration and data reduction will be the key to detailed analysis of potential variation of fundamental constants. The influence of calibration issues on the data quality is hard to measure and the magnitude of the resulting systematic error is under discussion. This work tries to bypass the estimation of systematics and utilizes the uncertainties as part of the analysis procedure.

¹ Program ID 68.A-0106.

² Program ID 68.B-0115(A).

2.3. Preprocessing

The first data set (henceforward referred to as set A) consists of nine separate spectra observed between 7th and 9th of January in 2002. The second set of 6 spectra (B) was obtained on January 13th in 2002. Prior to further data processing the reduced spectra are reviewed in detail.

2.3.1. Flux error level

The given error in flux of all 15 spectra was tested against the zero level noise in saturated areas. A broad region of saturated absorption is available near 3913 Å in the observers frame. Statistical analysis revealed a variance corresponding to ~120% of the given error on average for the 15 spectra. For each of the spectra the calculated correction factor was applied.

2.3.2. Relative shifts of the 15 spectra

Due to variation in barycentric velocities and grating shifts the individual spectra are subject to small shifts – commonly on sub-pixel level – in wavelength. To correct for that effect all spectra were interpolated by a polynomial using *Neville's algorithm* to conserve the local flux (see Fig. 1). The resulting pixel step on average is 1/20 of the original data. Each spectrum was compared to the others. For ev-

ery data point in a spectrum the pixel with the closest wavelength was taken from a second spectrum. Their deviation in flux was divided by the quadratic mean of their given errors in flux. This procedure was carried out for all pixels inside certain selected wavelength intervals³ resulting in a mean deviation of two spectra. The second spectrum is then shifted against the first one in steps of $\sim 1.5 \text{ m}\text{\AA}$. The run of the discrepancy of two spectra is of parabolic nature with a minimum at the relative shift with the best agreement. Fig. 2 shows the resulting curve with a parabolic fit. In this exemplary case the second spectrum shows a shift of $6.2 \text{ m}\text{\AA}$ in relation to the reference spectrum. The clean parabolic shape verifies the approach. All 15 spectra (A+B) are shifted to their common mean. The average deviation is $2.3 \text{ m}\text{\AA}$. Section 3.3 illustrates its influence on the data analysis.

2.3.3. Selection of lines

The selection of suitable H_2 features for the final analysis is highly subjective. As a matter of course all research groups crosschecked their choice of lines for unresolved blends or saturation effects. The decision whether a line was excluded due to continuum contamination or not, however, relied mainly on the expert knowledge of the researcher and was only partially reconfirmed by the ascertained uncertainty of the final fitting procedure. This work puts forward a more generic approach adapted to the fact that we have two distinct observations of the same object.

A selection of 52 lines is fitted separately for each dataset of 9 (A) and 6 (B) exposures, respectively. In this selection merely blends readily identifiable or emerging from equivalence width analysis are excluded. Each rotational level is fitted with conjoined line parameters except for redshift naturally. The data are not co added but analyzed simultaneously via the fitting procedure introduced by Quast et al. (2005). For each of the 52 lines there are

³ Only certain wavelength ranges are taken into account to avoid areas heavily influenced by cosmetics or areas close to overlapping orders.

two resulting fitted redshifts or observed wavelengths, respectively, with their error estimates. To avoid false confidence, the single lines are not judged by their error estimate but by their difference in wavelength between the two data sets in relation to the combined error estimate. Fig. 4 shows this dependency. The absolute offset $\Delta\lambda_{\text{effective}}$ to each other is expressed in relation to their combined error given by the fit:

$$\Delta\lambda_{\sigma_{\Sigma 1,2}} = \frac{\Delta\lambda_{\text{effective}}}{\sqrt{\sigma_{\lambda_1}^2 + \sigma_{\lambda_2}^2}}. \quad (1)$$

Fig. 4 reveals notable discrepancies between the two datasets, the disagreement is partially exceeding the $5\text{-}\sigma$ level⁴. Since the fitting routine is known to provide proper error estimates (Quast et al. 2005) and (Wendt & Reimers 2008), the dominating source of error in the determination of line positions is due to systematic errors. This result indicates calibration issues of some significance at this level of precision. The comparison of two independent observation runs reveals a source of error that can not be estimated by the statistical quality of the fit alone. For further analysis only lines that differ by less than 3σ are taken into account. This criterion is met by 36 lines. Fig. 3 shows three H_2 features corresponding to the transitions L5R1, L5P1, L5R2. All have similar sensitivity towards changes in μ . L5P1 fails the applied self consistency check between the two data sets and is excluded in the further analysis.

3. Results

For the final analysis the selected 36 lines are fitted in all 15 shifted, error-scaled spectra simultaneously. The result of an unweighted linear fit corresponds to $\Delta\mu/\mu = (15 \pm 16) \times 10^{-6}$ over the look-back time of $\sim 11.5 \text{ Gyr}$ for $z_{\text{abs}} = 3.025$. Fig. 5 shows the resulting plot.

⁴ Lines fitted with seemingly high precision and thus a low error reach higher offsets than lines with a larger estimated error at the same discrepancy in λ_{obs} . Clearly the lower error estimates merely reflects the statistical quality of the fit, not the true value of the specific line position.

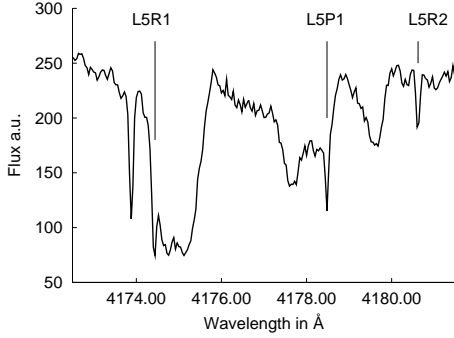


Fig. 3. Part of the co added spectrum near 4176Å. The data however, were not co added for the fit. L5R1 and L5R2 match the 3- σ criterion, L5P1 does not.

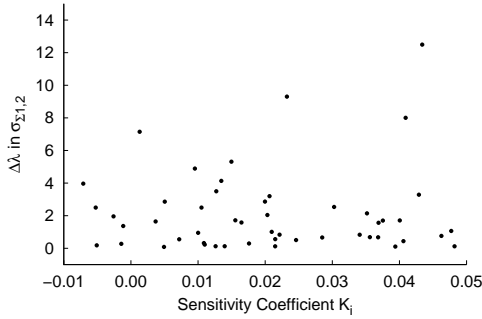


Fig. 4. Selection of 52 seemingly reasonable lines to be fitted separately for each dataset of 9 and 6 exposures, respectively. Their absolute offset $\Delta\lambda_{\text{effective}}$ to each other is expressed in relation to their combined error given by the fit (see Eq. 1).

Note the comparable large scatter in determined redshift when combining the two independent observations. The approach to apply an unweighted fit is a consequence of the unknown nature of the prominent systematics. Uncertainties in wavelength calibration can not be expressed directly as an individual error per line. For this work the calibration errors and the influence of unresolved blends are assumed to be dominant in comparison to individual fitting uncertainties per feature. For the following analysis the same error is adopted for each line. With an uncertainty in redshift of 1×10^{-6} we obtain: $\Delta\mu/\mu = (15 \pm 6) \times 10^{-6}$.

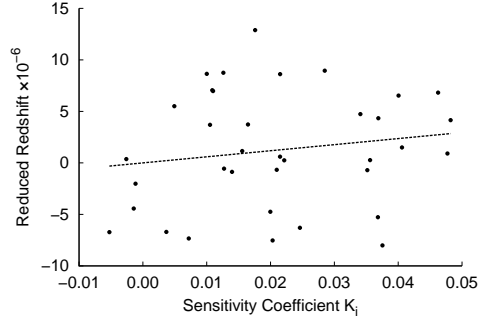


Fig. 5. The unweighted fit for Q0347 corresponds to $\Delta\mu/\mu = (15 \pm 16) \times 10^{-6}$. Note, that at such a high scatter $z_{K_i=0}$ differs from \bar{z} by less than $1 \sigma_z$.

However the goodness-of-fit is below 1 ppm and is not self consistent. Judging by that and Fig. 5, a reasonable error in observed redshift should at least be in the order of 5×10^{-6} . The weighted fit gives: $\Delta\mu/\mu = (15 \pm 14) \times 10^{-6}$.

3.1. Uncertainties in the sensitivity coefficients

At the current level of precision, the influence of uncertainties in the sensitivity coefficients K_i is minimal. It will be of increasing importance though when wavelength calibration can be improved by pedantic demands on future observations and eventually Laser Frequency Comb calibration will allow for practically arbitrary precision and uncertainties in the calculations of sensitivities will play a role. Commonly the weighted fits neglects the error in K_i . The χ^2 merit function for the case of a straight-line fit with errors in both coordinates is given by:

$$\chi^2(a, b) = \sum_{i=0}^{N-1} \frac{(y_i - a - bx_i)^2}{\sigma_{y_i}^2 + b^2 \sigma_{x_i}^2} \quad (2)$$

and can be solved numerically with valid approximations (Lybanon 1984). At the current level even an error in K_i of about 10% has merely impact on the error estimate in the order of 10^{-6} .

Alternatively the uncertainties in K_i can be

translated into an uncertainty in redshift via the previously fitted slope. The results of this ansatz are similar to the fit with errors in both coordinates and in general this is simpler to implement.

Another possibility is to apply a gaussian error to each sensitivity coefficient and redo the normal fit a few dozen times with alternating variations in K_i . Again, the influence on the error-estimate is in the order of 1 ppm.

The different approaches to the fit allow to estimate its overall robustness as well.

3.2. Individual line pairs

$\Delta\mu/\mu$ can also be obtained by using merely two lines that show different sensitivity towards changes in the proton-to-electron mass ratio. Another criterion is their separation in the wavelength frame to avoid pairs of lines from different ends of the spectrum. Several tests showed that a separation of $\Delta\lambda \leq 110\text{\AA}$ and a range of sensitivity coefficients $K_1 - K_2 \geq 0.02$ produces stable results that do not change any further with more stringent criteria. Note, that pairs spread across two neighboring orders ($\sim 50\text{\AA}$) show no striking deviations. Fig.7 shows the different values for $\Delta\mu/\mu$ derived from 52 line pairs that match the aforementioned criteria. Note, that a single observed line contributes to multiple pairs. The gain in statistical significance by this sorting is limited as pointed out by Molaro et al. (2008). The large scatter favors the median as result which produces $\Delta\mu/\mu = 13 \times 10^{-6}$. The scatter is then related to uncertainties in the wavelength determination which is mostly due to calibration errors. The standard error is 8×10^{-6} .

3.3. Influence of the preprocessing

Section 2.3.2 describes the initial shift to a common mean of all 15 spectra. The complete analysis was redone with error-scaled but unshifted spectra and the ascertained line positions of both runs compared. Fig. 6 shows the difference for each H_2 line in mÅ over the corresponding sensitivity coefficients K_i . The plotted line is a straight fit. Clearly the slope is

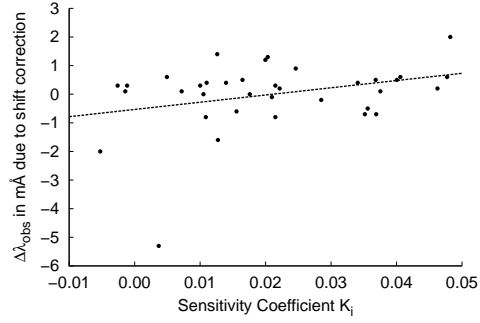


Fig. 6. Variation in fitted positions for all lines with and without initial correction for shifts in between the 15 spectra. The slope of the fit is dominated by three lines.

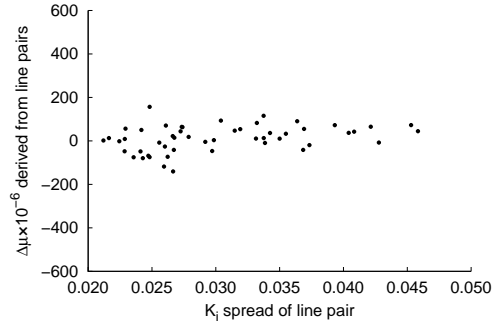


Fig. 7. $\Delta\mu/\mu$ derived from individual line pairs (52) which are separated by less than 110\AA and show a difference in sensitivity of more than 0.02. The median corresponds to $\Delta\mu/\mu = 13 \times 10^{-6}$.

dominated by three individual lines whose fitted centroids shifted up to 5.5 mÅ due to the preprocessing. These three lines in particular produce a trend towards variation in μ when grating shifts and other effects are not taken into account. This single-sided trend probably occurred by mere chance but at such low statistics it influences the final result.

Acknowledgements. We are thankful for the support from the Collaborative Research Centre 676 and for helpful discussions on this topic with S.A. Levshakov, P. Petitjean and M.G. Kozlov.

References

- Reinhold, E., et al. 2006, PRL, 96
King, J. A., et al. 2008, PRL, 101
Thompson, R. I., et al. 2009, APJ, 703, 2
Wendt, M. & Reimers, D. 2008, EPJ, 163, 197
Ivanchik, A., et al. 2005, A&A, 440, 45
Murphy, M. T., et al. 2008, MNRAS, 384, 1053
Quast, et al. 2005, A&A, 431, 1167
Lybanon, M. 1984, AJP, 52, 22
Molaro, P. et al. 2008, EPJ, 163, 173